Bull. Mater. Sci., Vol. 5, Nos 3 & 4, August & October 1983, pp. 287–306.

Transition metal chalcogenides exhibiting quasi-one-dimensional behaviour

J GOPALAKRISHNAN and K S NANJUNDASWAMY

Solid State and Structural Chemistry Unit, Indian Institute of Science, Bangalore 560 012, India.

Abstract. This paper presents a survey of transition metal chalcogenides (mainly sulphides and selenides) that exhibit unidimensional structural features and electronic properties arising therefrom. The survey indicates that linear, single-atom, chains of transition metals are formed in chalcogenides by sharing faces of MX_6 (X = chalcogen) trigonal prisms or octahedra as well as corners or edges of MX_4 tetrahedra. Besides these single-atom chain compounds, chalcogenides possessing multiple-atom chains are known among the early members of the transition series when the transition metal is in a low formal oxidation state. Typical examples of this class are Ti_5Te_4 and $TlMo_3Se_3$.

Keywords. Chalcogenides; transition metal compounds; one-dimensional solids; structures and properties

1. Introduction

Solids possessing anisotropic structural features such as layers or chains of atoms with weak interlayer or interchain bonding exhibit anisotropy in several of their physical properties. Among these so-called low-dimensional solids, those consisting of linear chains of metal atoms are of particular interest (Day 1983). The interest in one-dimensional metals dates back to the 1950s when Peierls (1955) showed from theoretical considerations the inherent instability of such systems with respect to periodic lattice distortion at low temperatures. The surge of recent interest in this area is however due to the availability of real materials exhibiting one-dimensional behaviour.

One-dimensional solids may be classified into two broad categories: one-dimensional *conductors* and one-dimensional *insulators*. Typical examples of one-dimensional conductors are TTF–TCNQ, $K_2Pt(CN)_4X_{0.3}3H_2O$ (X = Cl or Br), $NbSe_3$ and $BaVS_3$. Some of these systems, especially the first two, have been intensively investigated with respect to their structure, charge density wave (CDW) effects and electrical transport (Devreese *et al* 1979). One-dimensional insulators containing a chain of magnetic atoms are of special interest from the point of view of cooperative magnetic ordering and phase transition in one dimension (Birgeneau and Shirane 1978; Steiner *et al* 1976). Several insulating ABX_3 solids (A = Rb^+, Cs^+, Tl^+ or $(CH_3)_4N^+$; B = Mn^{2+}, Fe^{2+}, Co^{2+} or Ni^{2+} and X = Cl^-, Br^- or I^-) crystallize in a one-dimensional structure consisting of chains of B atoms. These chains are separated from one another by the large A cation. These solids exhibit quasi-one-dimensional magnetic behaviour, the prototype among them being $(CH_3)_4N\,MnCl_3$ (TMMC). TMMC is a one-dimensional Heisenberg antiferromagnet with an intrachain exchange energy,

Contribution No. 223 from the Solid State and Structural Chemistry Unit.

$J = -6{\cdot}3$ K; its magnetic behaviour is truly one-dimensional down to 0·84 K because of the large interchain separation (9·15 Å) (Ackerman *et al* 1974).

Several transition metal chalcogenides consisting of linear chains of metal atoms have been investigated in recent years. Many of them show properties associated with one-dimensional conductors and some of them are magnetic insulators exhibiting short-range ordering at low temperatures. A few of them such as $BaVS_3$ (Massenet *et al* 1978) show interesting magnetic and electrical properties attributable to the chain of metal atoms. A few chalcogenides consisting of a cluster of metal atoms that form linear chains by sharing cluster corners, edges or faces are also known (Simon 1981). While there are a number of reviews (Garito and Heeger 1974; Miller and Epstein 1976; Berlinsky 1979), monographs (Keller 1977; Devreese *et al* 1979) and conference reports (Subramanyam 1981) dealing in general with one-dimensional conductors and magnetic materials, studies relating to quasi-one-dimensional transition metal chalcogenides have not been reviewed in the literature excepting for the two recent reviews on transition metal trichalcogenides, mainly dealing with $NbSe_3$ and TaS_3 (Rouxel *et al* 1982; Meerschaut 1982). In this paper, we present a brief review of the structure, electrical transport, magnetic and related properties of quasi-one-dimensional transition metal chalcogenides, including our work in this area.

2. Transition metal trichalcogenides

Trisulphides and triselenides of Ti, Zr, Hf, Nb and Ta (MX_3) constitute a family of structurally related solids wherein the transition metal forms MX_6 trigonal prisms that share opposite faces resulting in MX_3 chains (Meerschaut 1982; Rouxel *et al* 1982). There are subtle differences between various members of this family arising from variations in X–X and M–M bonding which contribute to the rich variety of physical properties. Based on X–X bond length, three different structure types can be distinguished (table 1): (i) structure consisting of a single type of MX_3 chains, *e.g.* $ZrSe_3$; (ii) structure with two different MX_3 chains, *e.g.* $TaSe_3$ and (iii) structure with three different MX_3 chains, *e.g.* $NbSe_3$.

Trichalcogenides of Ti, Zr and Hf belong to the first group possessing a single type of MX_3 chains (figure 1) (Furuseth *et al* 1975). These crystallize in a monoclinic structure wherein the MX_3 chains run along the *b*-axis. One of the X–X distance in the MX_6 triangular prism base is quite short (2·05 Å in sulphides and 2·34 Å in selenides) revealing the formation of $[X\text{–}X]^{2-}$ species; accordingly the formal charges on the atoms are $M^{4+}(X_2)^{2-}X^{2-}$; this is consistent with their non-metallic nature. X-ray photoelectron spectroscopic (XPS) study (Jellinek *et al* 1976; Endo *et al* 1981, 1982) provides direct evidence for the presence of dichalcogenide as well as monochalcogenide species in these sulphides. NbS_3 (figure 2) also belongs to this structure type but in addition it shows a 2*b* superstructure (Rijnsdorp and Jellinek 1978). The superstructure arises from the formation of Nb–Nb bonds due to pairing of $Nb^{4+}: 4d^1$ electrons along the *b*-direction. The structure of NbS_3 has been regarded as the Peierls distorted insulating form of a one-dimensional metal. Rouxel *et al* (1981) attempted to detect an insulator-metal transition at high temperatures, but unfortunately the solid decomposes before it transforms to a metal. Cornelissens *et al* (1978) nevertheless found in an electron diffraction study that the spots associated with the 2*b* structure transform into streaks which is indicative of a decorrelation between the Nb chains; but a complete disappearance of streaks which would reveal a transition to the metallic

Table 1. Structures and properties of MX_3 trichalcogenides

MX_3	Structural information	Electrical and magnetic properties	References
MX_3 (M = Ti; X = S and M = Zr, Hf; X = S, Se, Te)	Monoclinic (figure 1)	Diamagnetic semiconductors	Furuseth *et al* (1975), Wilson (1979) and Meerschaut (1982).
NbS_3	Triclinic (figure 2); monoclinic at high pressure	Diamagnetic semiconductor, ρ at 300 K is 10^3 ohm-cm	Rijnsdorp and Jellineck (1978), Wilson *et al* (1979) and Kikkawa *et al* (1982).
$NbSe_3$	Monoclinic at ambient and high pressure	Two resistivity anomalies at 145 K and 59 K due to CDW formation, ρ at 300 K is $\sim 3 \times 10^{-3}$ ohm-cm.	Chaussy *et al* (1976), Hodeau *et al* (1978) Briggs *et al* (1980) and Kikkawa *et al* (1982).
TaS_3	Orthorhombic at ambient pressure and monoclinic at high pressure	Diamagnetic shows Peierls metal-insulator transition at 270 K. ρ at 300 K is $\sim 8 \times 10^{-2}$ ohm-cm.	Bjerkelund and Kjekshus (1964), Meerschaut *et al* (1981), Roucau *et al* (1980) and Kikkawa *et al* (1982).
$TaSe_3$	Monoclinic at ambient and high pressure	Superconducting below 2·2 K	Bjerkelund *et al* (1966), Yamamoto (1978) and Kikkawa *et al* (1982).
MoS_3	Amorphous with a chain structure consisting of Mo–Mo pairs; $Mo^{5+}\ (S_2^{2-})_{\frac{1}{2}}\ (S^{2-})_2$; $Mo^{2+}\ S_3^{2-}$	Diamagnetic semiconductor; ρ at 300 K is $\sim 3{\cdot}8 \times 10^4$ ohm-cm.	Liang *et al* (1980), Murugesan and Gopalakrishnan (1982) and Chianelli (1982).
WS_3	Amorphous similar to MoS_3	Diamagnetic semiconductor; ρ at 300 K is $\sim 5{\cdot}2 \times 10^4$ ohm-cm	Chianelli (1982).

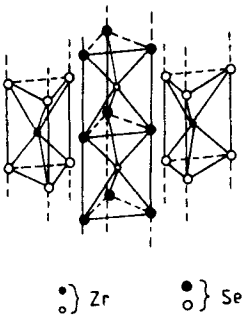

Figure 1. Structure of $ZrSe_3$.

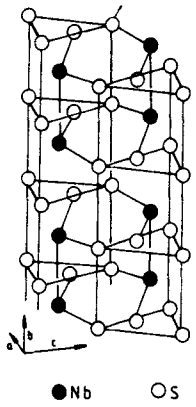

Figure 2. Structure of NbS_3. Nb–Nb bonds are shown.

state has never been observed.

An example of a trichalcogenide possessing two different kinds of trigonal prismatic MX_3 chains is $TaSe_3$ (Bjerkelund *et al* 1966). In one chain, the Se–Se bond length is 2·58 Å, slightly longer than the Se–Se single bond length (2·35 Å); in the other chain, the Se–Se distance is 2·91 Å indicating that the Se atoms are nearly nonbonded. These differences in Se–Se bond lengths have been taken to indicate that the formal oxidation state of tantalum is intermediate between 4+ and 5+ in these chains. In the first chain, it is likely to be closer to 4+ and in the second it may be more close to 5+. The material is metallic conducting, undergoing a transition to superconducting state at $\sim 1{\cdot}5$ K (Hean *et al* 1978).

The structure of $NbSe_3$ is the most complex of all the MX_3 chalogenides, consisting of three different types of trigonal prismatic chains with different Se–Se distances, 2·37, 2·48 and 2·91 Å (Hodeau *et al* 1978). Accordingly the oxidation state of niobium in the first chain is likely to be 4+, in the second intermediate between 4+ and 5+ and in the third it is nearly 5+. In other words, the differences in Se–Se bond lengths reflect the differences in electron concentration available at the niobium atom in the various chains.

$NbSe_3$ shows an unusual metallic behaviour with two resistivity anomalies at 145 and 59 K (figure 3). These anomalies are due to formation of CDW's representing opening up of gaps in the Fermi suface (Meerschaut 1982; Rouxel *et al* 1982). The increase in resistivity at 145 and 59 K has been attributed to a decrease in the Fermi surface. Specific heat anomalies at these temperatures have been noticed and the associated entropy changes ΔS are $0{\cdot}01R$ at 145 K and $\sim 0{\cdot}005R$ at 59 K. Pressure removes the resistivity anomalies. In addition, the material becomes a superconductor at $\sim$ 6 kbar when the CDW's are suppressed. More strikingly, $NbSe_3$ shows nonohmic electrictal transport, the magnitude of both the resistivity anomalies decreasing with increasing current. There is a threshold field above which nonlinearity sets in. Different models have been proposed to explain the unusual electrical transport behaviour of $NbSe_3$. One of the models due to Bardeen (1979) attributes the nonohmic conductivity of $NbSe_3$ to a Zener type tunnelling through a pinning potential.

TaS_3 is known in two forms, orthorhombic and monoclinic, of which the latter is

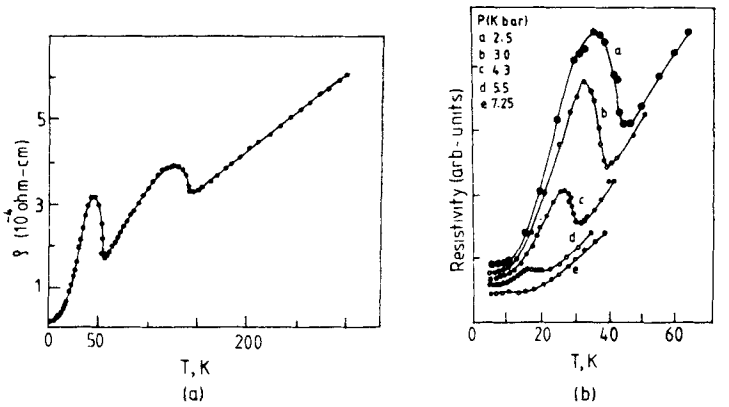

Figure 3. (a) Resistivity-temperature plots for $NbSe_3$. (b) Resistivity-temperature plots for $NbSe_3$ at various pressures.

structurally similar to $NbSe_3$ with three different kinds of chains (Meerschaut *et al* 1981). Monoclinic TaS_3 also shows two electrical transitions at 240 and 160 K; the first one appears to be a metal-insulator transition of the Peierls type (Meerschaut *et al* 1979). Superlattice spots due to CDW effects in the electron diffraction pattern are seen around these transition temperature (Roucau *et al* 1980). Like $NbSe_3$, TaS_3 also shows nonohmic behaviour. Orthorhombic TaS_3, whose structure is not yet known, also shows a metal-insulator transition around 210 K. In general, these transition metal trichalcogenides exhibit several properties that are characteristic of low-dimensional materials: intercalation, CDW fluctuations and nonlinear effects. However the exact dimensionality is difficult to define and may vary from case to case. For instance, TaS_3 is more one-dimensional than $NbSe_3$ probably because of the larger ionicity of the Ta–S bond than the Nb–Se bond. Another interesting aspect of these trichalcogenides, especially of Group V metals, is the variable X–X bond length. These bond lengths determine the electron density available at the metal chains. A large X–X length would indicate transfer of electrons from the transition metal to the chalcogen. Accordingly, the chains exhibiting longest X–X bond lengths would probably be insulating in $NbSe_3$ and TaS_3, while those chains with shortest X–X bonds corresponding to Nb^{4+} or Ta^{4+} states account for the metallic conductivity, CDW and other associated properties.

Unlike Group IV and Group V trichalcogenides, MoS_3 and WS_3 are known only in the amorphous state (Murugesan and Gopalakrishnan 1982). Structural investigations making use of X-ray scattering, EXAFS and XPS have shown that these materials also possess chain-like structures with metal-metal bonded pairs (Chianelli 1982).

There have been attempts to modify the structure and electronic density of these trichalcogenides by substitution of first row transition metal atoms. In this process, a new one-dimensional material, $FeNb_3Se_{10}$, has been synthesized (Hillenius *et al* 1981). There are two types of metal chains in this chalcogenide, one, trigonal prismatic chain of $NbSe_3$ type with a short Se–Se distance of 2·348 Å and the other, an octahedral chain containing both Fe and Nb atoms (Cava *et al* 1981). $FeNb_3Se_{10}$ is metallic showing a giant electrical transition around 140 K with a change of 9 orders of magnitude in resistivity. Superstructure spots in the electron diffraction reveal the formation of CDW states below 140 K similar to that in $NbSe_3$. $FeNb_3Se_{10}$ represents a new one-

dimensional structure type and it should be possible to synthesize interesting materials of this type by substitution of other first row transition metals in $NbSe_3$.

3. One-dimensional iron sulphides

Iron forms a number of ternary sulphides with strongly electropositive alkali and alkaline-earth metals. Several of them possess one-dimensional structures, the well-known among them being $AFeS_2$ (A = K, Rb or Cs) (Bronger 1981). $NaFeS_2 \cdot 2H_2O$ occurs as a mineral (Erdite) and has recently been synthesized (Boller and Blaha 1983). All these four sulphides are structurally related possessing linear chains of FeS_4 tetrahedra formed by sharing two opposite edges of each tetrahedron. The $[FeS_{4/2}]_\infty$ chains, which are similar to SiS_2, are held together by the A cations. There are, nevertheless, minor differences in the structures of different members arising from variable size of the A cations. Mixed-valence iron sulphides, $Na_3Fe_2S_4$ and $Tl_3Fe_2S_4$, possessing the same linear $[FeS_{4/2}]_\infty$ framework, are also known (Klepp and Boller 1981; Sabrowsky *et al* 1979). Crystal structures of some of these sulphides are given in figure 4 and the data are summarized in table 2.

A remarkable property of these sulphides is that the A cations are easily exchangeable by divalent cations such as Ca^{2+}, Sr^{2+} and Ba^{2+}. Boller (1978) has prepared

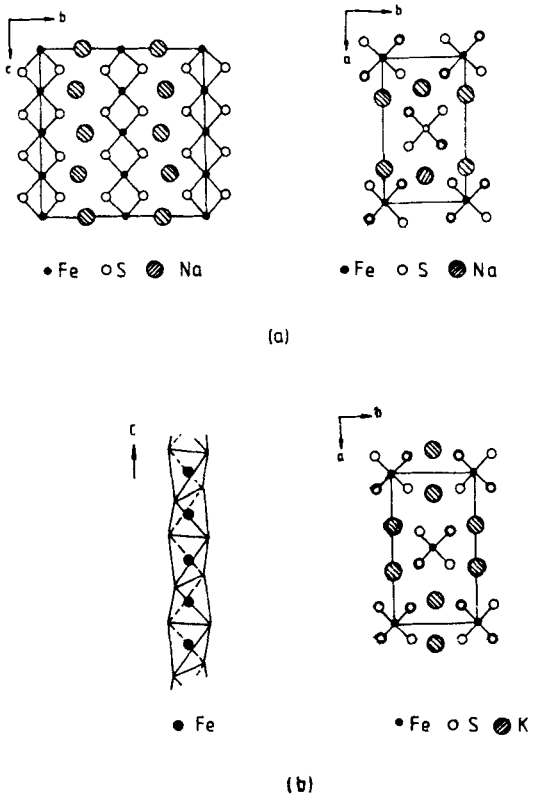

Figure 4. Structure of $AFeS_2$: (a) $NaFeS_2$ (b) $KFeS_2$.

Table 2. Structure and properties of $AFeS_2$

$AFeS_2$	Crystallographic data		M–M bond distance along the chain (Å)	Magnetic properties	References
$NaFeS_2$	Orthorhombic: Space group *I*222 $Z = 4$	$a = 6{\cdot}25$ $b = 10{\cdot}83$ $c = 5{\cdot}40$ Å	2·70	Shows linear-chain antiferromagnetism similar to $KFeS_2$	Boller and Blaha (1983).
$Na_3Fe_2S_4$	Orthorhombic: Space group *Pnma* $Z = 4$	$a = 6{\cdot}633$ $b = 10{\cdot}675$ $c = 10{\cdot}677$ Å	2·745		Sabrowsky *et al* (1979), Klepp and Boller (1981)
$KFeS_2$	Monoclinic: Space group *C*2/*c* $Z = 4$	$a = 7{\cdot}09$ $b = 11{\cdot}27$ $c = 5{\cdot}39$ Å $\beta = 112° 30'$	2·70	Show linear-chain	Boon and MacGillary (1942),
$RbFeS_2$	Monoclinic: Space group *C*2/*c*	$a = 7{\cdot}22$ $b = 11{\cdot}70$ $c = 5{\cdot}42$ Å $\beta = 112{\cdot}2°$	2·71	antiferromagnetism. Three-dimensional ordering of moments takes place below 250K ($KFeS_2$)	Sweeney and Coffman (1972), Nishi and Ito (1979), Swinnea and Steinfink (1982) and
$CsFeS_2$	Orthorhombic: Space group *Immm* $Z = 4$	$a = 7{\cdot}13$ $b = 11{\cdot}92$ $c = 5{\cdot}42$ Å	2·696 2·725	188K ($RbFeS_2$) and 66K ($CsFeS_2$) respectively	Bronger and Muller 1980, Bronger 1981.

$Ca(FeS_2)_2 \cdot xH_2O$, $Sr(FeS_2)_2 \cdot xH_2O$, $Ba(FeS_2)_2$ and so on by ion exchange method starting from $KFeS_2$,

$$2KFeS_2 + M^{2+} + xH_2O \longrightarrow M(FeS_2)_2 \cdot xH_2O + 2K^+.$$

These phases are formed topochemically, retaining the one-dimensional $[FeS_{4/2}]_\infty$ framework. This is revealed by the lattice constants of the ion-exchanged phases, which show changes only in the *a*-parameter, the *c*-parameter remaining nearly constant around 5·5 Å.

One-dimensional iron sulphides possessing linear chains of FeS_4 tetrahedra similar to $AFeS_2$ are also known in the Ba–Fe–S system (Grey 1974). These sulphides with the general formula $Ba_{1+x}Fe_2S_4$ are prepared by high temperature ($\sim 800°C$) reaction of BaS, Fe and S. A recent study of the system (Swinnea and Steinfink 1982) has shown that series of phases possessing *infinitely adaptive structures* exist in the composition range $0{\cdot}072 \leqslant x \leqslant 0{\cdot}142$. Within this composition range, no biphasic region exists indicating that every possible composition attains a fully ordered structure; the phases in this composition range may therefore be considered an infinitely adaptive series. It is significant that $BaFe_2S_4$ itself is not a member of this series. Structures of several members of the series, $Ba_p(Fe_2S_4)_q$, for various values of p and q have been determined (Grey 1975; Hoggins and Steinfink 1977). The structures of these solids are built up of two subcells, one consisting of $[FeS_{4/2}]_\infty$ and the other chains of Ba atoms as in $KFeS_2$. Since $p \neq q$ in the series, the periodicity of the structure is repeated every pth barium (*oop*) layer or every qth sulphur (*ooq*) layer. According to Hoggins and Steinfink (1977), the Ba and Fe_2S_4 subcells exhibit $I4/mmm$ and $I4/mcm$ symmetry. When the two subcells are packed together in $Ba_p(Fe_2S_4)_q$ members, the space group symmetry changes depending on the combinations of p and q: when p = odd and q = even, the space group is $P4/mnc$; when p = even and q = odd, the space group is $P4/mcc$ and when both p and q are odd, the space group is $I4/m$. Idealized structures of some of the members of this series are illustrated in figure 5.

Magnetic and electrical properties of some of these one-dimensional iron sulphides have been studied (Sweeney and Coffman 1972; Swinnea and Steinfink 1982). Stoichiometric $AFeS_2$ and $BaFe_2S_4$ are linear chain antiferromagnets exhibiting semiconducting behaviour. Typically, these sulphides show small magnetic susceptibilities that are weakly dependent on temperature. The $\chi_m^{-1} - T$ plot (figure 6) for $KFeS_2$ is nearly temperature independent from 100 to 300 K and then slopes gently downward revealing a maximum at a much higher temperature. The data indicate that

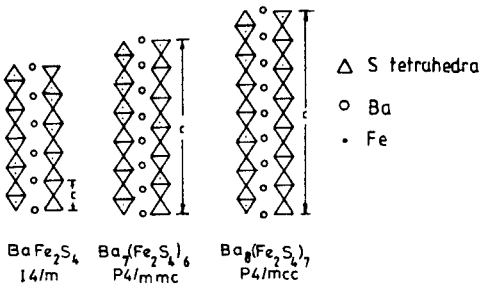

Figure 5. Idealized models of structures of $Ba_p(Fe_2S_4)_q$ members.

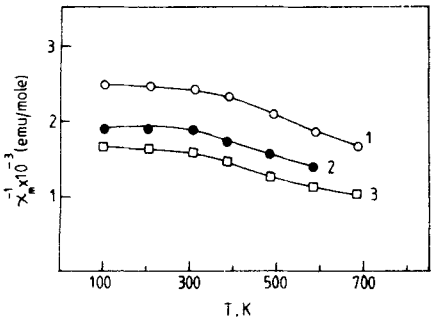

Figure 6. $\chi_m^{-1} - T$ plots for $AFeS_2$: 1, $KFeS_2$; 2, $RbFeS_2$; and 3, $CsFeS_2$.

the iron atoms are strongly coupled antiferromagnetically along the chain and fit qualitatively into a Heisenberg model for linear chain antiferromagnetism with $J = -286$ K.

Mössbauer effect studies (Taft and Danon 1975) of $AFeS_2$ have shown small isomer shifts (0·18–0·19 mm/sec) that are characteristic of tetrahedral site iron (III) in sulphides. A neutron diffraction study of $KFeS_2$ (Nishi and Ito 1979) has confirmed that the spins are antiferromagnetically coupled along the $[FeS_{4/2}]_\infty$ chain direction and ferromagnetically coupled in planes containing *a*- and *b*-axes below 250 K. The iron moment ($2{\cdot}43 \pm 0{\cdot}03\ \mu_B$ at 4·2 K and $2{\cdot}37 \pm 0{\cdot}03\ \mu_B$ at 77 K) is only about half of what is expected for high-spin Fe^{3+}: $3d^5$ ($S = 5/2$). The low value is consistent with the low hyperfine field measured by Mössbauer spectroscopy (Scorzelli *et al* 1978).

Electrical and magnetic properties of $Ba_{1+x}Fe_2S_4$ have been studied by Swinnea and Steinfink (1982). Stoichiometric $BaFe_2S_4$ is a semiconductor (room temperaure conductivity 5×10^{-7} ohm^{-1} cm^{-1}) with $E_g = 0{\cdot}66$ eV. In contrast, non-stoichiometric $Ba_{1+x}Fe_2S_4$ members are better conductors (room temperature conductivities are around 10^{-2} ohm^{-1} cm^{-1}) with low activation energies (0·017–0·065 eV). The magnetic behaviour of stoichiometric $BaFe_2S_4$ (figure 7a) is similar to that of $KFeS_2$, the susceptibility varying slowly with temperature; the data do not show a Curie–Weiss behaviour but seem to fit a classical $S = 5/2$ Heisenberg Hamiltonian with $J/k = -30$ K.

The magnetic behaviour of both $BaFe_2S_4$ and $KFeS_2$ has been attributed to antiferromagnetic superexchange interaction between Fe^{3+} ions along the edge-shared $[FeS_{4/2}]_\infty$ chains (Swinnea and Steinfink 1982). The infinite chain of Fe^{3+} ions (Fe–Fe separation = 2·7 Å) results in two *d*-bands, one for α-spin electrons and the other for β-spin electrons. In $KFeS_2$ and $BaFe_2S_4$, the α-spin *d*-band is completely filled and the β-spin *d*-band is empty. For this ground state, no effective magnetic moment is expected. The weak moments experimentally seen are attributed to electrostatic repulsion between the α-spin electrons causing a residual localization of electrons at Fe^{3+}.

The magnetic behaviour of $Ba_{1+x}Fe_2S_4$ (figure 7b) is different from that of $BaFe_2S_4$, showing a Curie–Weiss temperature dependence of susceptibility. The $\chi_m^{-1} - T$ plot is linear above 140 K and shows an incipient ferrimagnetic ($\theta = 265°$ K) ordering. The effective magnetic moment of 2·07 B.M. calculated from the linear region of the $\chi_m^{-1} - T$ plot arises from the β-spin electrons of Fe^{2+} created by the nonstoichiometric

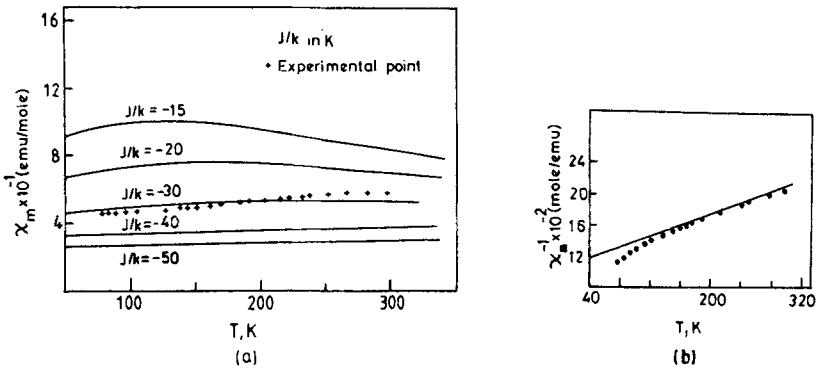

Figure 7. (**a**) Comparison between the experimental values of susceptibility for $BaFe_2S_4$ (+) and calculated values from Heisenberg model ($S = 5/2$) for various J/k values. (**b**) $\chi_m^{-1} - T$ plot for $Ba_{1\cdot091}Fe_2S_4$. The linear portion of the curve gives $\mu_{eff} = 2\cdot07$ BM and $\theta = -265°K$.

excess of xBa in $Ba_{1+x}Fe_2S_4$.

In an attempt to evaluate the magnetic property of isolated Fe^{3+} in tetrahedral sulphur coordination, the magnetic properties of $CsGa_{1-x}Fe_xS_2$ members have been investigated (Bronger and Müller 1980). Upto $x \sim 0\cdot45$, the members of the series crystallize in the monoclinic structure of $CsGaS_2$. The magnetic susceptibility data of these members reveal that for small values of $x(0\cdot01)$, the iron moment corresponds to the 'spin-only' $S = 5/2$ state, while for larger values of x, the moment becomes smaller reaching $1\cdot81\ \mu_B$ at $x \sim 0\cdot45$. The result seems to indicate that the spin state of iron changes from $S = 5/2$ (high spin) to $S = 1/2$ (low spin) with increasing x in the $CsGa_{1-x}Fe_xS_2$ system. These workers have also found that the magnetic interactions in $CsFeS_2$ is strongly perturbed by grinding the samples. Whereas crystalline $CsFeS_2$ shows the expected linear chain antiferromagnetic behaviour, finely powdered $CsFeS_2$ shows a Curie–Weiss temperature dependence of susceptibility with a magnetic moment of $1\cdot7\ \mu_B$.

4. $BaVS_3$ and related chalcogenides

$BaVS_3$ is the prototype of a family ternary chalcogenides of the general formula $BaMX_3$ (M = Ti, V, Nb or Ta and X = S or Se) exhibiting quasi-one-dimensional structure and properties (table 3). $BaVS_3$ crystallizes at room temperature in the $CsNiCl_3$ structure (space group $P6_3/mmc$) consisting of linear chains of vanadium atoms formed by face sharing VS_6 octahedra (figure 8). Barium atoms are surrounded by twelve sulphur atoms in the structure and essentially serve the purpose of isolating the vanadium chains. A short intrachain V–V distance (2·805 Å) and a fairly long interchain V–V separation (6·724 Å) ensure unidimensionality of the structure and V–V interactions (Gardner *et al* 1969).

$BaVS_3$ shows two phase transitions, one at 240 K and the other at 80 K. These transitions have been investigated by Gardner *et al* (1969), Takano *et al* (1977), Massenet *et al* (1978), Ghedira *et al* (1981) and Sayetat *et al* (1982). The 240 K transition is a crystallographic transition in which the crystal symmetry of stoichiometric $BaVS_3$

Table 3. Structure and properties of $BaMX_3$

$BaMX_3$	Crystallographic data	M–M intra-chain distance (Å)	M–M inter-chain distance (Å)	Electrical and magnetic properties	References
$BaTiS_3$	Hexagonal: $a = 6{\cdot}730$, $c = 5{\cdot}829$Å; Space group $P6_3/mmc$	2·914	6·730	Diamagnetic insulator	Hahn and Mutschke (1956), Clearfield (1963)
$BsVS_3$	High temperature phase: Hexagonal, $a = 6{\cdot}7253$, $c = 5{\cdot}6263$Å; Space group $P6_3/mmc$, $Z = 2$. Low temperature phase: Orthorhombic, $a_o \simeq a_h$, $b_o \simeq \sqrt{3}a_h$, $c_o \simeq c_h$; Space group $Cmc2_1$ or $C222_1$, $Z = 4$	2·8813	6·725	At 240 K $BaVS_3$ transforms from hexagonal to orthorhombic structure, the paramagnetic metallic $BaVS_3$ transforms to non-magnetic non-metallic state at 80 K. Stoichiometric $BaVS_3$ order antiferromagnetically at 70 K; whereas sulfur defecient $BaVS_3$ orders ferromagnetically at 16 K.	Gardner *et al* (1969), Takano *et al* (1977), Massenet *et al* (1978), Wada *et al* (1980), Ghedira *et al* (1981) and Sayetat *et al* (1982)
$BaVSe_3$	Hexagonal: $a = 6{\cdot}999$, $c = 5{\cdot}862$Å; Space group $P6_3/mmc$	2·931	6·999	Shows ferromagnetic ordering at 41°K and transforms to orthorhombic structure at 303° K.	Kelber *et al* (1979)
$BaNb_{0{\cdot}8}S_3$	Hexagonal: $a = 6{\cdot}831$, $c = 5{\cdot}764$Å; Space group $P6_3/mmc$	2·882	6·831	Semiconductor	Aslanov (1964)
$BaTa_{0{\cdot}8}S_3$	Hexagonal: $a = 6{\cdot}826$, $c = 5{\cdot}776$Å; Space group $P6_3/mmc$	2·888	6·826	Semiconductor	Aslanov and Kovba (1964), Gardner *et al* (1969), Donohue and Weiher (1974)
$BaTa_{0{\cdot}8}Se_3$	Hexagonal: $a = 7{\cdot}108$, $c = 6{\cdot}030$Å; Space group $P6_3/mmc$	3·015	7·108	Semiconductor	

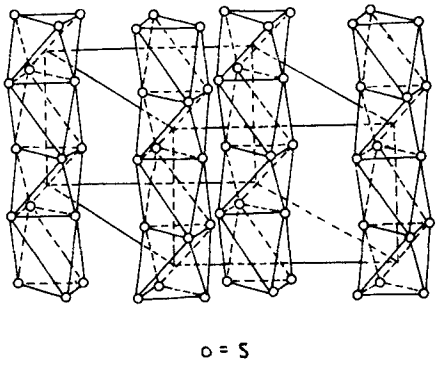

Figure 8. One-dimensional chains of face-sharing VS_6 octahedra in $BaVS_3$. Hexagonal cell is also shown.

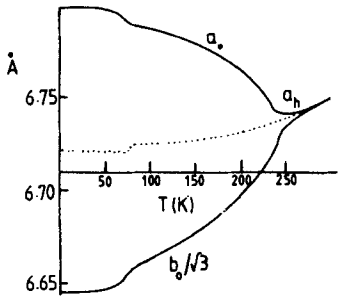

Figure 9. Variation of a_0, $b_0/\sqrt{3}$ (orthorhombic) and a_h (hexagonal) parameters with temperature. The dotted curve represents variation of $(a_0 b_0/\sqrt{3})^{1/2}$.

changes from hexagonal ($P6_3/mmc$) to orthorhombic ($Cmc2_1$ or $C222_1$) with $a_0 \simeq a_h$, $b_0 \simeq \sqrt{3}a_h$ and $c_0 \simeq c_h$. The major structural change accompanying this transition is that the linear vanadium chains along c_h become zigzag chains around c_0 in the orthorhombic phase. From the changes in unit cell parameters (figure 9), it has been suggested that the transition is of a second-order displacive type. At the second transition which occurs at 80 K, there is no change in crystal symmetry; but there is a discontinuity in the a_0 and b_0 parameters and not in the c_0 parameter.

$BaVS_3$ shows dramatic changes in electrical and magnetic properties as a function of temperature (Massenet *et al* 1978). The magnetic behaviour is strongly influenced by sulphur stoichiometry. Stoichiometric $BaVS_3$ shows a quasi-one-dimensional antiferromagnetic behaviour with a broad maximum in the susceptibility around 70 K (figure 10). Sulphur-deficient $BaVS_3$, on the other hand, shows a ferromagnetic ordering with $T_c = 16$ K (figure 9). The susceptibility behaviour above 80 K of both the samples are Curie–Weiss like with an effective magnetic moment of 1·17 μ_B which is significantly lower than the value expected for a V^{4+}: $3d^1$ system. Both stoichiometric and sulphur-deficient $BaVS_3$ behave as poor metals above 150 K. Resistivity (figure 11) increases by about six orders of magnitude reaching a maximum around 70 K, where the susceptibility is also a maximum. The data indicate that the second phase transition

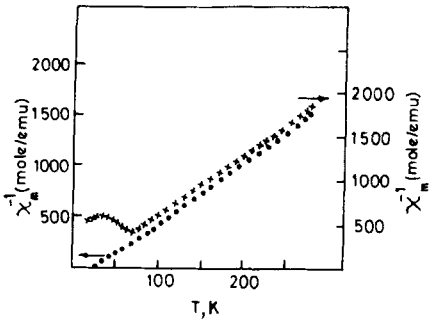

Figure 10. $\chi_m^{-1} - T$ plots for stoichiometric (xxx) and sulphur-defecient (. . . .) $BaVS_3$.

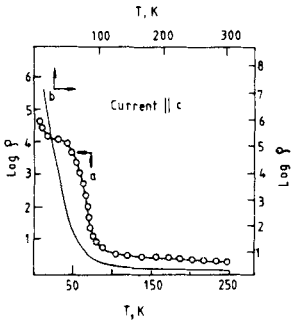

Figure 11. Log $\rho - T$ plots for stoichiometric (–) and sulphur-defecient (·····) single crystals of $BaVS_3$.

around 80 K is a electric-magnetic transition at which stoichiometric $BaVS_3$ goes from a Curie–Weiss paramagnetic and metallic state to a nonmagnetic and nonmetallic state. It is to be emphasized that the transition is not of the Peierls type since the vanadium atoms of the zigzag chains in the orthorhombic phase remain equidistant and no V–V pairs are formed below 80 K.

A theoretical model to explain the complex behaviour of $BaVS_3$ is still lacking. Massenet *et al* (1979) proposed a qualitative two-band model to explain the structure and properties of $BaVS_3$. The octahedral-site V^{4+} in VS_6 octahedra, which form linear chains, gives rise to two bands derived from the vanadium 3*d*-states; one is a narrow band of t_{2g} parentage and the other, a broad one, derived from strong overlap of d_{z^2} orbitals along the chain. The simultaneous presence of metallic conductivity and localized magnetic moment is the result of an overlap between the broad and narrow bands as shown in figure 12. The metallic behaviour is due to the d_{z^2} electrons, while the magnetic properties arise from the t_{2g} electrons. The model, however, fails to rationalize convincingly the transition to a nonmagnetic nonmetallic state below 80 K. Takano *et al* (1977) attributed the electrical transition at 80 K to a Slater-mechanism (Slater 1951) involving antiferromagnetic coupling of V–V atoms along the chain.

Massenet *et al* (1979) studied the solid solution series $BaV_xTi_{1-x}S_3$. Phases isostructural with the parent $BaVS_3$ and $BaTiS_3$ have been obtained over the entire range $0 \leqslant x \leqslant 1$. The c/a ratio decreases progressively from 0·866 at $BaTiS_3$ to 0·838 at

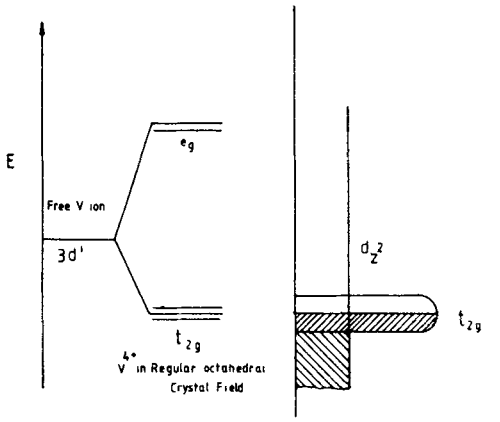

Figure 12. Schematic band model for the electronic structure of $BaVS_3$.

$BaVS_3$. While there is a transition from semiconducting behaviour to metallic behaviour with increasing x, resistivity becomes anomalously large at $x \sim 0{\cdot}2$. Wada *et al* (1980) who studied the same system found that the hexagonal-to-orthorhombic transition of $BaVS_3$ is suppressed by titanium substitution, the transition being totally absent when the titanium concentration exceeds 40 mol%.

$BaVSe_3$, isostructural with $BaVS_3$, has been prepared (Kelber *et al* 1979). It also undergoes a transition to orthorhombic structure at 303 K. $BaVSe_3$ is paramagnetic down to 41 K, where it orders ferromagnetically with a moment of $0{\cdot}2\ \mu_B$ per vanadium atom. Further studies are required to fully characterize the structural and electronic transitions in this phase. We have recently prepared a sample of $SrVS_3$ that crystallizes in orthorhombic structure at room temperature ($a_0 = 6{\cdot}744$, $b_0 = 11{\cdot}652$ and $c_0 = 5{\cdot}820$ Å). A study of its electronic properties is in progress.

A number of $BaMX_3$ phases analogous to $BaVS_3$ have been reported in the literature (Aslanov 1964; Aslanov and Kovba 1964; Gardner *et al* 1969; Donohue and Weiher 1974). Gardner *et al* (1969) reported that $BaTaS_3$ is isostructural with $BaVS_3$, but semiconducting instead of being metallic. Donohue and Weiher (1974), who subsequently studied the system found that the correct composition of the phase is $BaTa_{0{\cdot}8}S_3$ rather than $BaTaS_3$, implying that the valency of tantalum is 5+ in the compound thus accounting for the semiconducting behaviour. Phases with similar composition and structure have been reported in the Ba–Nb–S and Ba–Ta–Se systems. Recently Swinnea *et al* (1983) prepared a barium-niobium-sulphide of approximate composition $Ba_4Nb_2S_9$ which crystallizes in a rhombohedral structure consisting of columns of three NbS_6 octahedra that share opposite faces. It is not a one-dimensional compound since there are no continuous Nb–Nb chains in this structure.

5. Ba_2MX_3 and related chalcogenides

The chalcogenides of Ba_2MX_3 ($M = Mn^{2+}, Fe^{2+}, Co^{2+}, Zn^{2+}$; X = S, Se) crystallize in chain structures isostructural with K_2AgI_3 or K_2CuCl_3 (Wells 1975). The structures essentially consist of MS_4 tetrahedra that share each two corners to form linear chains

$[MS_2S_{2/2}]_\infty$, the barium atoms packing in between the chains; the intrachain M–M distance ($\sim$ 4·3 Å) is considerably shorter than the interchain M–M distance ($\sim$ 6.1 Å) conferring a dominant M–M interaction along the chains in these compounds (Grey and Steinfink 1971). These chalcogenides are insulators possessing fairly high resistivities at room temperature (10^4 ohm cm; E_a = 0·6 eV for Ba_2FeS_3). Magnetic susceptibility measurements have shown that the manganese, iron and cobalt compounds in the series exhibit quasi-one-dimensional antiferromagnetic short-range ordering in the chains (Nakayama *et al* 1980). A reduced-spin model based on the Ising model has been used to fit the magnetic susceptibility data. The magnetic data together with unit cell parameters of these sulphides are summarized in table 4.

The intrachain exchange energy J/k of these sulphides is considerably greater than the value for the halides such as $CsMnCl_3$. This has been attributed to (Grey and Steinfink 1971) a larger superexchange (covalency), M–X–M, in the chalcogenides than the halides. In view of the large intrachain M–M separation ($\sim$ 4·5 Å) in these compounds, contribution from direct exchange to the exchange energy is regarded to be much smaller than the superexchange *via* the bridging chalcogenides.

Mössbauer spectrum of Ba_2FeS_3 down to 77 K shows (Nakayama *et al* 1980) a large quadrupole splitting which is typical of high-spin Fe^{2+}. The fact that the spectrum does not change at 77 K is consistent with one-dimensional short-range antiferromagnetic ordering. At 4·2 K, the spectrum shows magnetic splitting indicating that three-dimensional long-range ordering sets in due to interchain interactions.

The present authors have prepared a series of quaternary metal sulphides of the general formula La_3MAlS_7 (M = Mn, Fe, Co) consisting of linear chains of face shared MS_6 octahedra and isolated AlS_4 tetrahedra (Nanjundaswamy and Gopalakrishnan 1983). From the structure (figure 13) (Flahaut and Laruelle 1970) it is expected that the magnetic interaction among M ions is restricted to the chains. Susceptibility measurements (figure 14) reveal linear chain antiferromagnetic behaviour similar to Ba_2MS_3 phases.

6. Metal cluster chain compounds

A common feature of all chalcogenides discussed so far is that they possess single atom chains formed by sharing corners or edges of MX_4 tetrahedra (as in Ba_2FeS_3 or $KFeS_2$) as well as sharing faces of MX_6 octahdera or trigonal prisms (as in $BaVS_3$ or $NbSe_3$). In contrast, a new class of metal-chain chalcogenides are known where the chain consists of multiple atoms formed by condensation of metal cluster units. A typical example of this family is Ti_5Te_4 (Grønvold *et al* 1961) in which octahedral Ti_6 units condense through opposite corners to give a one-dimensional column structure (figure 15). Octahedral M_6 cluster can also condense through sharing opposite edges, and corners as well as faces. The existence of a bewildering array of such low-dimensional solids among the metal-rich chalcogenides of the early transition metal series has come to be recognized in recent times; the subject is reviewed by Simon (1981, 1982). A particularly significant series of chalcogenides belonging to this class is MMo_3X_3 (M = Na, K, Rb, Cs, In, Tl; X = S, Se, Te) which consists of infinite chains of face condensed octahedral Mo_6 clusters; these can be regarded as derived from MMo_6X_8 Chevrel phases (Hönle *et al* 1980; Potel *et al* 1980). These compounds crystallize in the hexagonal $TlFe_3Te_3$ structure (Klepp and Boller 1979) wherein the

Table 4. Structure and properties of Ba_2MX_3

Ba_2MX_3	Crystallographic data		M–M intra-chain distance (Å)	J/k the inter-action energy (K) from reduced spin model	Effective magnetic moment (μ_{eff}) from reduced spin model (BM)	References
Ba_2MnS_3	Orthorhombic: Space group *Pnma* Z = 4	a = 8·814 b = 4·302 c = 17·048 Å	4·30	−12	6·42	Grey and Steinfink (1971), Hong and Steinfink (1972) and Nakayama *et al* (1980)
Ba_2MnSe_3	Orthorhombic: Space group *Pnma*	a = 9·135 b = 4·471 c = 17·736 Å	4·47	−9·6	—	Grey and Steinfink (1971)
Ba_2FeS_3	Orthorhombic: Space group *Pnma*	a = 12·087 b = 4·246 c = 12·359 Å	4·25	−20·5	5·20	Hong and Steinfink (1972), Reiff *et al* (1975) and Nakayama *et al* (1980)
Ba_2FeSe_3	Orthorhombic: Space group *Pnma*	a = 12·350 b = 4·439 c = 12·921 Å	4·44	—	—	Hong and Steinfink (1972)
Ba_2CoS_3	Orthorhombic: Space group *Pnma*	a = 11·87 b = 4·20 c = 12·30 Å	4·20	−15	4·35	Hong and Steinfink (1972), Nakayama *et al* (1980).

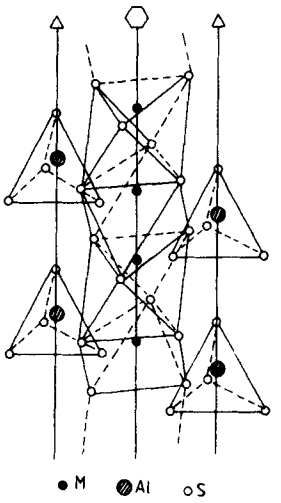

Figure 13. Structure of La_3MAlS_7 (M = Mn, Fe, Co). Only MS_6 octahedra forming chains and isolated AlS_4 tetrahedra are shown.

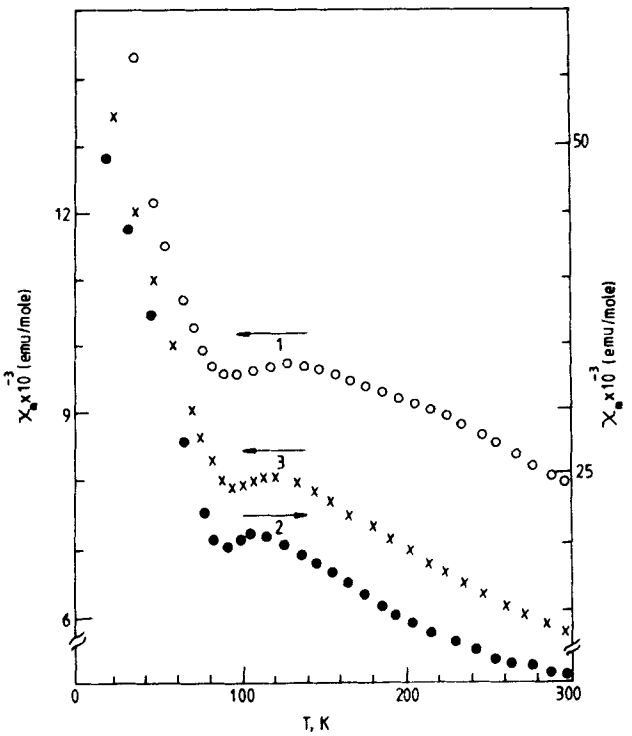

Figure 14. $\chi_m - T$ plots for La_3MAlS_7: 1, M = Mn; 2, M = Fe; and 3, M = Co.

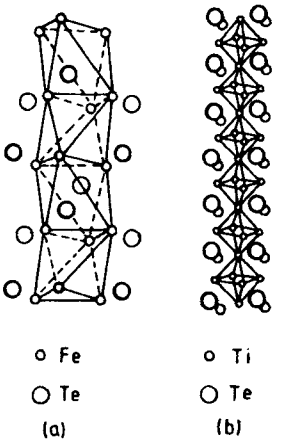

Figure 15. Structures of metal cluster chain compounds: (**a**) $TlFe_3Te_3$:Fe_6 octahedra share opposite faces. (**b**) Ti_5Te_4:Ti_6 octahedra share opposite corners.

infinite chains of condensed metal cluster run parallel to the *c* axis. As expected, these solids exhibit anisotropic physical properties. The electrical resistivity of $TlMo_3Se_3$ for example is 30 μohm cm at 4·2 K parallel to the *c* axis, while the resistivity perpendicular to *c* is several hundred times larger. At 3·5 K, the solid becomes superconducting. Recently Hughbanks and Hoffmann (1982) presented a band model for the electronic structure of $[Mo_3Se_3^-]_\infty$ chain. According to this model, the topmost band is of Mo–Mo anti-bonding a_2 type which is half-filled for $Mo_3Se_3^-$ unit. Accordingly, one predicts a Peierls distortion and semiconducting ground state at low temperatures. However, $TlMo_3Se_3$ is superconducting at low temperatures. The anomaly has been attributed to the participation of Tl^+ levels which perturbs the simple 'one-dimensional' picture. KMo_3Se_3 appears to conform to this model showing a semiconducting ground state at low temperatures.

7. Concluding remarks

In this review, we have presented a survey of transition metal chalcogenides (mainly sulphides and selenides) that exhibit unidimensional structural features and electronic properties arising therefrom. The survey indicates that linear single-atom, chains of transition metals are formed by sharing corners or edges of MX_6 tetrahedra as well as faces of MX_6 octahedra or trigonal prisms. There seems to be a correlation between the electrical and magnetic properties on the one hand and the oxidation state of the transition metal (M) atom on the other in these chalcogenides. When the M atom is in a high oxidation state as in $NbSe_3$ and $TaSe_3$, the M–X–M interaction along the chain is sufficiently strong to give rise to unidimensional metallic conductivity and related CDW phenomena at low temperatures. Divalent first row-transition metal (Mn, Fe, Co) chalcogenides are generally insulators and exhibit short-range antiferromagnetic ordering along the chains. With intermediate oxidation states, the metal-chain compounds tend to exhibit both localized magnetism and metallic conductivity as in $BaVS_3$ and $Ba_{1+x}Fe_2S_4$. Besides these single-atom chain compounds, chalcogenides

consisting of multiple-atom chains are known among the metal-rich chalcogenides of the early members of the transition series wherein the transition metal is in a low oxidation state. Multiple-atom chains in these chalcogenides are formed by condensation of metal–metal bonded cluster units. Typical examples of this class of compounds are Ti_5Te_4 and $TlMo_3Se_3$.

Acknowledgement

Grateful thanks of the authors are due to Professor C N R Rao, F.R.S for helpful suggestions and encouragement.

References

Ackerman J F, Cole G M and Holt S L 1974 *Inorg. Chim. Acta* **8** 323
Aslanov L A 1969 *Russ. J. Inorg. Chem.* **9** 1090
Aslanov L A and Kovba L M 1964 *Russ. J. Inorg. Chem.* **9** 1317
Bardeen J 1979 *Phys. Rev. Lett.* **42** 1498
Berlinsky A J 1979 *Rep. Prog. Phys.* **42** 1243
Birgeneau R J and Shirane G 1978 *Phys. Today* (December)
Bjerkelund E and Kjekshus A 1964 *Z. Anorg. Allg. Chem.* **328** 235
Bjerkelund E, Fermer J H and Kjekshus A 1966 *Acta Chem. Scand.* **20** 1836
Boller 1978 *Monatsch. Chem.* **109** 975
Boller H and Blaha H 1983 *Monatsch. Chem.* **114** 145
Boon J W and MacGillary C H 1942 *Recl. Trav. Chim. Phys.-Bas* **61** 910
Briggs A, Monceau P, Nunez-Regueiro M, Peyrard J, Ribault M and Richard J (1980) *J. Phys.* **C13** 2117
Bronger W and Müller P 1980 *J. Less-Common Metals* **70** 253
Bronger W 1981 *Angew. Chem.* **20** 52 and references therein
Cava R J, Hines V L, Mighell A D and Roth R S 1981 *Phys. Rev.* **B24** 3634
Chaussy J. Haen P, Lasjaunias J C, Monceau P, Waysand G, Waintal A, Meerschaut A, Molinie P and Rouxel J 1976 *Solid State Commun.* **20** 759
Chianelli R R 1982 *Int. Rev. Phys. Chem.* **2** 127
Clearfield A 1963 *Acta Crystallogr.* **16** 134
Cornelissens T, Van Tendeloo G, Van Landuyt J and Amelinckx S 1978 *Phys. Status Solidi.* **A48** K5
Day P, 1983 *Chem. Bri.* **19** 306
Devreese J T, Evrard R and Van Doren U E V 1979 *Highly conducting one-dimensional solids* (New York: Plenum)
Donohue P C and Weiher J D 1974 *J. Solid State Chem.* **10** 142
Endo K, Ihara H, Watanabe K and Gonda S 1981 *J. Solid State Chem.* **39** 215
Endo K, Ihara H, Watanabe K and Gonda S 1982 *J. Solid State Chem.* **44** 268
Flahaut J and Laruelle 1970 *The chemistry of extended defects in non-metallic solids* (eds) L Eyring and M O'Keeffe (Amsterdam: North-Holland) p. 109
Furuseth S, Brattas L and Kjekshus A 1975 *Acta Chem. Scand.* **29** 623
Gardner R, Vlasse M and Wold A 1969 *Acta Crystallogr.* **B25** 781
Garito A F and Heeger A J 1974 *Acc. Chem. Res.* 7 232
Ghedira M, Chenavas J, Sayetat F, Marezio M, Massenet O and Mercier J 1981 *Acta Crystallogr.* **B37** 1491
Grey I E 1974 *J. Solid State Chem.* **11** 128
Grey I E 1975 *Acta Crystallogr.* **B31** 45
Grey I E and Steinfink H 1971 *Inorg. Chem.* **10** 691
Grønvold F, Kjekshus A and Raaum F 1961 *Acta Crystallogr.* **14** 930
Hean P, Lapierre F, Monceau P, Nunez-Regueiro M and Richard J 1978 *Solid State Comm.* **26** 725
Hahn H and Mutschke U 1956 *Z. Anorg Chem.* **288** 269
Hillenius S J, Coleman R V, Fleming R M and Cava R J 1981 *Phys. Rev.* **B23** 1567
Hodeau J L, Marzio M, Roucau C, Ayroles R, Meerschaut A, Rouxel J and Monceau P 1978 *J. Phys.* **C11** 4117

Hoggins J T and Steinfink H 1977 *Acta Crystallogr.* **B33** 673
Hong H Y and Steinfink H 1972 *J. Solid State Chem.* **5** 93.
Hönle W, Von Schnering H G, Lipka A and Yvon K 1980 *J. Less-Common Metals* **71** 135
Hughbanks T and Hoffman R 1982 *Inorg. Chem.* **21** 3578
Jellinek F, Pollack R A and Shafer M W 1976 *Mater. Res. Bull.* **9** 845
Kelber J, Reis Jr. A H, Aldred A T, Muller M H, Massenet O, DePasquali G and Stucky G 1979 *J. Solid State Chem.* **30** 357
Keller H J 1977 *Chemistry and physics of one-dimensional metals* (New York: Plenum)
Kikkawa S, Ogawa N, Koizumi M and Onuki Y 1982 *J. Solid State Chem.* **41** 315
Klepp K and Boller H 1979 *Monatsh. Chem.* **110** 677
Klepp K and Boller H 1981 *Monatsch. Chem.* **112** 83
Liang K S, de Neufville J P, Jacobson A J, Chianelli R R and Betts F 1980 *J. Non-Cryst. Solids* **35, 36** 1249
Massenet O, Buder R, Sinee J J, Schlenker C, Mercier J, Kelber J and Stucky D G 1978 *Mater. Res. Bull.* **13** 187
Massenet O, Sinee J J, Mercier J, Avignon M, Buder R, Nguyen V D and Kelber J 1979 *J. Phys. Chem. Solids* **40** 573
Meerschaut A 1982 *Ann. Chim. Fr.* **7** 131
Meerschaut A, Guemas L and Rouxel J 1981 *J. Solid State Chem.* **36** 118
Meerschaut A, Rouxel J, Haen P, Monceau P and Nunez-Regueiro M 1979 *J. Phys. Lett.* **62** 483
Miller J S and Epstein A J 1976 *Prog. Inorg. Chem.* **20** 1
Murugesan T and Gopalakrishnan J 1982 *Proc. Indian Acad. Sci. (Chem. Sci.)* **91** 7 and the references therein.
Nakayama N, Kosuge K, Kachi S, Shinjo T and Takada T 1980 *J. Solid State Chem.* **33** 351
Nanjundaswamy K S and Gopalakrishnan J 1983 *J. Solid State Chem.* (in print)
Nishi M and Ito Y 1979 *Solid State Commun.* **30** 571.
Peierls R E 1955 *Quantum theory of solids* (Oxford: University Press)
Potel M, Chevrel R, Sergent M, Armici J C, Decroux M and Fisher Ø 1980 *J. Solid State Chem.* **35** 286
Reiff W M, Grey I E, Fan A, Eliezer Z and Steinfink H 1975 *J. Solid State Chem.* **13** 32
Rijnsdorp and Jellinek 1978 *J. Solid State Chem.* **25** 325
Roucau C, Ayroles R, Monceau P, Guemas L, Meerschaut A and Rouxel J 1980 *Phys. Status. Solidi.* **A62** 483
Rouxel J, Meerschaut A, Guemas L and Gressier P 1982 *Ann. Chim. Fr.* **7** 445
Sabrowsky H, Mirza J and Chr. Methfessel 1979 *Z. Naturforsch,* **B34** 115
Sayetat F, Ghedira M, Chenavas J and Marezio M 1982 *J. Phys.* **C15** 1627
Scorzelli R B, Taft C A, Danon J and Garg V J 1978 *J. Phys.* **C11** L 397
Simon A 1982 *Angew. Chem.* **20** 1
Simon A 1982 *Ann. Chim. Fr.* **7** 539
Slater J C 1951 *Phys. Rev.* **83** 538
Steiner M, Villian J and Windsor C G 1976 *Adv. Phys.* **25** 7
Subramanyam S V 1981 in *Preparation and characterization of materials* (eds) J M Honig and C N R Rao (New York: Academic Press) p. 367
Sweeney W V and Coffman R E 1972 *Biochim. Biophys. Acta* **286** 16
Swinnea J S and Steinfink H 1982 *J. Solid State Chem.* **41** 114, 124
Swinnea J S, Steinfink H, Rendon-Diazmiron L E and Gomezdaza M 1983 *J. Solid State Chem.* **46** 367
Taft C A and Danon J 1975 *J. Phys. Chem. Solids* **36** 283
Takano M, Kosugi H, Nakanishi N, Shimada M, Wada T and Koizumi M 1977 *J. Phys. Soc. Jpn* **43** 1101
Wada T, Shimada M and Koizumi M 1980 *J. Solid State Chem.* **33** 357
Wells A F 1975 *Structural inorganic chemistry* Fourth Edition (Oxford: University Press)
Wilson J A 1979 *Phys. Rev.* **B19** 6456
Yamamota M 1978 *J. Phys. Soc. Jpn* **45** 431